Landscape Ecology **17:** 157–171, 2002.

A leakiness index for assessing landscape function using remote sensing

John A. Ludwig[1,*], Robert W. Eager[2], Gary N. Bastin[3], Vanessa H. Chewings[3] and Adam C. Liedloff[2]

*[1]Tropical Savannas Management Cooperative Research Centre and CSIRO Sustainable Ecosystems, PO Box 780, Atherton, 4883, Queensland, Australia; [2]Tropical Savannas Management Cooperative Research Centre and CSIRO Sustainable Ecosystems, Darwin, 0822, Northern Territory, Australia; [3] Alice Springs, 0871, Northern Territory, Australia; *Author for correspondence (e-mail: john.ludwig@cse.csiro.au)*

Received 30 August 2000; accepted in revised form 8 October 2001

Key words: Landscape metrics, Patch cover, Patch orientation, Patch size, Spatial pattern, Tropical savanna, Vegetation patchiness

Abstract

The cover, number, size, shape, spatial arrangement and orientation of vegetation patches are attributes that have been used to indicate how well landscapes function to retain, not 'leak', vital system resources such as rainwater and soil. We derived and tested a directional leakiness index (DLI) for this resource retention function. We used simulated landscape maps where resource flows over map surfaces were directional and where landscape patch attributes were known. Although DLI was most strongly related to patch cover, it also logically related to patch number, size, shape, arrangement and orientation. If the direction of resource flow is multi-directional, a variant of DLI, the multi-directional leakiness index (MDLI) can be used. The utility of DLI and MDLI was demonstrated by applying these indices to three Australian savanna landscapes differing in their remotely sensed vegetation patch attributes. These leakiness indices clearly positioned these three landscapes along a function-dysfunction continuum, where dysfunctional landscapes are leaky (poorly retain resources).

Introduction

Patches of vegetation serve an important function in many desert, grassland and savanna landscapes around the world by capturing and retaining limited resources such as rainwater, organic matter, and soil sediments and nutrients (Tongway and Ludwig 1997a). This function is confirmed by landscape studies documenting 'islands of fertility' within a matrix of infertility (e.g., Anderson and Hodgkinson (1997); Burke et al. (1999); Cross and Schlesinger (1999); Reid et al. (1999)), and by studies relating runoff and soil losses to vegetation patch cover (e.g., Johns (1983); Lang and McCaffrey (1984); McIvor et al. (1995); Galle et al. (1999)). Landscapes with many vegetation patches covering their surfaces will efficiently retain and utilize resources (Tongway and Ludwig 1997a). These landscapes are conserving or highly functional systems, whereas landscapes with few such patches are leaky or dysfunctional (Tongway and Ludwig 1997b). Landscapes occur along a theoretical continuum of functionality from highly patchy systems that conserve all resources to those that have no patches and leak all resources (Ludwig and Tongway 2000). Few landscapes would occur at these extremes, of course, but this continuum is useful for comparing the functionality (leakiness) of landscapes subject to different disturbances (e.g., Ludwig et al. (2000a)).

Directly measuring how efficiently landscapes capture, retain and cycle water and nutrients, hence reduce runoff and erosion, is very costly in terms of field and laboratory time (e.g., Scanlan et al. (1996); Burke et al. (1999); Galle et al. (1999); Schlesinger et al. (2000)). Thus, simple indicators that reflect these landscape processes and functions are used (Tongway and Ludwig 1997b). These indicators include the cover, number and mean size of perennial vegetation patches, which are attributes that can be obtained by remote sensing (e.g., Ludwig et al.

(2000b)). In addition to these simple patch measures, field and modelling studies have shown that the shape and spatial orientation and arrangement of patches within a landscape can also influence how efficiently water and nutrients can be retained and utilized for plant production (e.g., Reynolds et al. (1997); Cross and Schlesinger (1999); Ludwig et al. (1999a)).

These patch measures have mostly been used as separate indicators to compare landscapes (e.g., Tongway and Ludwig (1997b)). However, these measures are obviously related (e.g., patch cover increases as the number of patches increases if patch size remains constant). Therefore, it seems logical to integrate these patch measures into simple indicators of landscape function. For example, a 'weighted mean patch size' index has been derived from the number of patches and their mean size to describe landscape structure (Li and Archer 1997). Others have combined patch size and configuration to derive indices of landscape fragmentation and heterogeneity (e.g., Li and Reynolds (1994); Jaeger (2000)). The lacunarity index has been used to compare landscape patch patterns such as degree of segregation (Wu and Sui 2001) and patch functions such as connectivity of surface flows (Wu et al. 2000), and how darkling beetles use patches (McIntyre and Wiens 2000). However, no one simple index has been derived that logically relates landscape function (resource retention) to separate indicators (i.e., patch cover, number, size, shape and spatial arrangement and orientation).

In this paper, we derive a directional leakiness index, DLI, that logically relates to all these landscape patch attributes, thus providing a simple indicator of landscape function (resource retention). We tested the sensitivity of this index, and a multi-directional variant, MDLI, to these patch attributes. We first used spatial modelling to generate maps where patch attributes were known. Then, to demonstrate the usefulness of DLI, we applied it to three remotely-sensed savanna landscapes that differed in their state of dysfunction.

Principles for a leakiness index

Rather than deriving a landscape leakiness index directly from remotely-sensed patch cover, number, size, shape and spatial arrangement attributes by trying to combine all these attributes into a complex mathematical equation, we returned to first principles of how landscape processes function to retain resources flowing across surfaces. Envisage resources such as litter and soil particles loosely sitting on an open, relatively uniform landscape surface (e.g., between patches of vegetation on low-relief landforms in a desert, grassland or savanna), and then having these litter and soil particles blown across this surface in the direction of the prevailing wind or being carried by runoff (sheet-flow) in the direction of the slope. Clearly, these organic, soil and water resources will flow across the open landscape surface until they hit an obstruction that traps them (Tongway and Ludwig 1997a; Reid et al. 1999; Schlesinger et al. 2000), or until they flow out of the landscape system of interest (Ludwig et al. 2000a). Surface obstructions are typically vegetation patches of various types and sizes, for example, clumps of grass, shrub thickets and groves of trees, but obstructions may also include logs, rocks, ant and termite mounds, and soil banks or cracks and pits (see examples in Whisenant (1999)).

Landscapes that have a high cover of these obstructions have a high potential for capturing any resources blowing or flowing across their surfaces (Tongway and Ludwig 1997b). If obstructing patches are close together and uniformly dispersed, then litter and soil particles and runoff are likely to only move a short distance from any open surface before being trapped within a patch (Cross and Schlesinger 1999). However, if these patches are few and far apart (i.e. have a low cover), then particles and runoff are much more likely to gain the energy they need to blow or flow (leak) out of the landscape system (Pressland and Lehane 1982; Leys 1991).

From these principles, we derived a landscape leakiness index with four important properties: (1) applicable to remotely-sensed landscape images; (2) scaleable to a standard map area so that different sized images can be compared; (3) applicable to landscapes where the direction of resource flow is known, and if not, then a simple variant applies; and (4) ranges from 0 to 1 for non-leaky to totally leaky landscapes.

Maps and standard areas

The landscape leakiness index we derived applies to raster-based (pixel) maps from images obtained by remote sensing (Figure 1a). Each pixel in the map is classified as being patch or non-patch (Figure 1b). Adjoining patch pixels form patches (potentially, resource trapping obstructions) and groups of non-patch

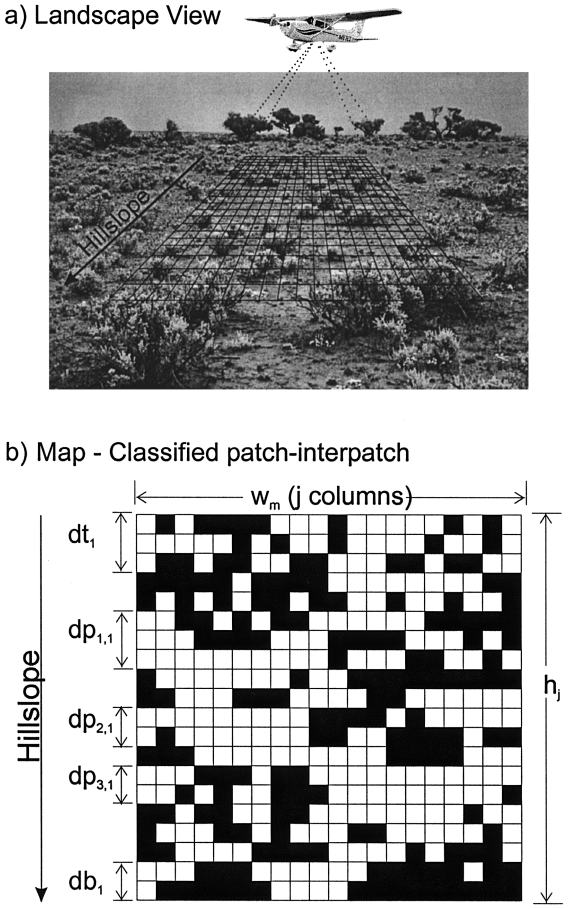

Figure 1. Schematic of a hillslope landscape: (a) being remotely sensed and (b) as a map where each pixel is classified as being either a flow obstructing patch (solid squares) or non-obstructing interpatch (open squares). Distances shown down the first column (j = 1) of this map are for top and bottom edges (dt_1 and db_1) and for between patches (e.g., $dp_{1,1}$). If square pixels are assumed to have a dimension of 1 m, then the height of columns (h_j) is 20 m and the width of the map (w_m) is 20 m.

pixels form interpatches (gaps or openings between patches). Typically such classified maps are obtained by processing images from aerial videography or satellites (e.g., Pickup et al. (1993, 2000)), however, simulation modelling can also be used to generate spatial maps (e.g., Gardner (1999)). In this study, we used both remotely-sensed landscape maps and simulated spatial maps to derive and test our leakiness index.

Ideally, an index should be directly comparable across study sites differing in area or scale. To make the leakiness index developed in this paper comparable across sites, we recommend scaling it to a standard area, which should vary according to the pixel size of the remotely sensed imagery used. For pixels of 1 m or less, as typically used by low-level aerial videography, we recommend the use of a square of 100 m×100 m (1 ha) as the standard area. If pixels are larger than 1 m, but not more than 10 m, such as from high-resolution satellite or airborne imagery, use a 1 km×1 km area. If pixels are greater than 10 m, as typical with Landsat Multi Spectral Scanner (MSS) or Thematic Mapper (TM), sattellite imagery then use a 10 km×10 km area as the standard. Of course, the pixel size and imagery used in landscape function (resource retention) studies must be able to distinguish flow-obstructing patches from open interpatches; imagery with large pixels will fail to do this in vegetation types with fine-scale patches (see Discussion).

Scaling the leakiness index to a standard area of, for example, 1 ha can be viewed as a question. What would be the value of the leakiness index if we had sampled a 100 m×100 m area that has the *same* percent cover, size, spacing and arrangement of patches as the area we actually sampled? For example, assume we had produced a 20 m×20 m classified spatial map from a aerial videography image (e.g., Figure 1b), and we wanted to compare the potential leakiness of this landscape map to that for a 100 m×100 m (1 ha) landscape map. To do this, we need to computationally standardize our 20 m×20 m leakiness index to that for a 100 m×100 m area that is conceptualized as having the *same* patch characteristics (see Appendix).

Directional leakiness

A directional leakiness index (DLI) applies when we assume that the general direction of resource flow across a landscape is known. For example, on a hillslope, the flow of soil sediments in runoff will be in the downhill direction (Figure 1a). Also on this hillslope, litter and soil particles will tend to blow in the direction of prevailing winds. These slope and wind directions may be the same, but if not and both flows are of interest, then DLI can be determined separately for water-driven and wind-driven flows. If the direction of these flows is unknown, then a variant of DLI, the multi-directional leakiness index (MDLI) applies (see section, “Multi-directional leakiness index”).

The directional leakiness index DLI is computed as:

$$DLI = 1 - [(L\text{max} - L\text{obs})/(L\text{max} - L\text{min})]^k \quad (1)$$

The term in square brackets raised to the k power indicates the potential of a landscape to retain resources. To indicate leakiness, this retention term must be subtracted from one (i.e., leakiness = 1−retention). DLI ranges from 0 (no leakiness) to 1 (totally leaky) as resource retention ranges from 1 (full retention) to 0 (no retention). This range is achieved by dividing the estimated retention (*Lmax–Lobs*) by the maximum possible retention (*Lmax–Lmin*).

Observed leakiness (*Lobs*) is a measure of the relative leakiness of the sample area scaled to a standard area (e.g., 1 ha). This *Lobs* is based on three distances within each column, j, of the sample map (Figure 1b): (1) the distance from the top edge of the column to the first patch (dt_j), (2) the distance from the last patch in the column to the bottom edge (db_j), and (3) the distances between patches, i, ($dp_{i,j}$) down column j. These distances are in units of meters, calculated as the number of pixels times pixel dimension (pd, in meters).

Given these distances, the observed leakiness component in Equation (1) is calculated as:

$$L_{\text{obs}} = \sum_j [(h_s/h_j)\cdot(\sum_i dp_{i,j}^2) + ((h_s/h_j) - 1)\cdot((dt_j + db_j)^2) + (dt_j^2 + db_j^2)]\cdot(w_s/w_m)\cdot(pd) \quad (2)$$

The terms in this equation are described in detail in a Appendix. The reason distances are raised to a power of 2 is because of the known nonlinear relationship between interpatch opening size and wind- and water-driven erosive energies (Williams 1978; Findlater et al. 1990; Leys 1991). Although we used the power of 2, other powers could be used if erosive energies were known.

Scaling from the sample area to a standard area involves using proportional dimensions. This scaling is achieved by multiplying certain distance terms in Equation (2) by the ratios h_s/h_j and w_s/w_m, where h_s and w_s are the height and width of the standard area (in meters), and where h_j is the column height and w_m is the map width of the sample area (also in meters).

The second component required to compute DLI is maximum possible leakiness, *Lmax*. This component is required to have DLI range from 0 to 1. *Lmax* is simply the calculation of *Lobs* for a spatial map exhibiting maximum leakiness, which occurs when the map has no obstructing patch pixels. If this map is a 100×100 m standard area, then $Lmax = 100^2$ summed for 100 columns = 1,000,000.

The third component, also needed to have DLI range from 0 to 1, is minimum leakiness, *Lmin*. For the purposes of this paper, we have simply assumed that *Lmin* = 0. However, one can set *Lmin* to a value greater than 0 (see Discussion).

The parameter k in Equation (1) determines the steepness of the decay curve formed when DLI is plotted against the proportion of a spatial map covered by patch pixels. It is known that resource leakiness (e.g., soil loss) rapidly declines (decays away) as the ground cover of vegetation patches (e.g., perennial grass tussocks) increases up to about 40%, with soil loss slowly declining at higher ground covers (Scanlan et al. 1996). We calculated several series of DLI's using differing k values and compared these to decay curvature data for soil loss versus vegetation ground cover from Scanlan et al. (1996), and from many other Australian field studies (Pressland and Lehane 1982; Johns 1983; Lang and McCaffrey 1984; Leys 1991; Miles and McTainsh 1994; McIvor et al. 1995; Carroll and Tucker 2000). We used curve-fitting procedures in SigmaPlot (SPSS Inc. 2000) and obtained a good fit of DLI to all this decay curve data with $k = 5$. One can, of course, vary k to fit DLI to soil loss versus ground cover data for a specific study, but our aim here was to describe a general relationship using such data from many studies; this was achieved with $k = 5$.

Multi-directional leakiness index

In some cases the direction a litter or soil particle blows or flows before hitting an obstruction in the landscape is unknown. For example, in many Australian landscapes with low relief, the level of resolution of topographic contour lines or digital elevation models is inadequate to accurately determine the direction of slope. This is true for many of the flat landscapes that have been studied with aerial videography (e.g., Kinloch et al. (2000)). Wind records are also very sparse in many areas, making estimates of prevailing wind directions imprecise.

In the case of uncertain flow direction, a multi-directional leakiness index, MDLI, is computed as a simple variant of DLI by using a sequential procedure linking MDLI to DLI. Although automated 'Euclid-

ean distance' procedures in spatial analysis packages could have been used for these assumed multi-directional flows (e.g., Gardner (1999)), such distance procedures that seek the closest patch pixel (in any direction) from a non-patch pixel do not adhere to our logic for directional wind- and water-driven landscape leakiness flows. Further, linking MDLI to DLI also provides information about patch shape/spatial configurations that might exist in the landscape (see below).

Without any attempt to orientate the spatial map, which for these multi-directional calculations we recommend be a square or rectangular area with c columns and r rows, MDLI is calculated by first computing a DLI for columns (Equation 1); this DLI is designated DLIc. This calculation for DLIc could be down columns or up columns in the spatial map (either way, the squared distance sums would be the same; see Equation (1)). Second, a DLIr was computed by similarly calculating along rows of the map. Then, DLIc and DLIr were averaged to obtain a MDLI for the map:

$$MDLI = (DLI_c + DLI_r)/2 \quad (3)$$

Modelled maps and leakiness

Landscape maps were generated using spatial modelling procedures (e.g., Gardner (1999)). These procedures were used to generate 1 ha maps of 100 by 100 pixels with each pixel 1 m in dimension. Maps were varied in the proportion (%) of the map covered by patch pixels and in the number and size of patches formed by these pixels. The shapes of these patches were varied (from single squares to bands), and the spatial pattern of these patches was also varied (random, regular and clustered). To explore how DLI and MDLI relate to these different landscape patch attributes, we varied some attributes while the other attributes were held constant or were varied proportionally.

First, using a random pattern (Figure 2a), the total cover of patches was increased from 0 to 100% by increasing the number of patch pixels from 0 to 10,000 (in this case, mean patch size must also increase). We found that with random pixel placement, DLI sharply decreased as the cover of patches increased (Figure 3a). This strong response, where DLI is most sensitive at low patch covers, makes this index very useful for indicating landscape leakiness because landscapes with very low vegetation cover rapidly lose (leak) soil by wind- and water-driven forces (e.g., Miles and McTainsh (1994); Scanlan et al. (1996)). Such landscapes have been termed dysfunctional (Tongway and Ludwig 1997b; Ludwig and Tongway 2000). In this case, where patch pixels were randomly placed, DLI and MDLI were approximately equal (i.e., DLIr $\approx$ DLIc; Figure 2a), as would be expected.

Using a regular pattern (Figure 2b), the number of patches was increased by decreasing patch size (i.e., smaller groups of patch pixels in squares), while the cover of patch pixels was held constant (e.g., at 10%). DLI decreased as the number of patches increased (Figure 3b), and as cover was increased to 20% the curve shifted down, as expected (i.e., leakiness decreased as patch cover increased). Again, DLI $\approx$ MDLI, and these curves have the desired indicator response shape because litter and soil resources move about more in landscapes with a few large vegetation patches than in those with many small patches that more uniformly cover the landscape (e.g., Reynolds et al. (1997); Cross and Schlesinger (1999)).

Using clustered patterns of patches (Figure 2c), the compactness of patch clusters was varied from very tight to loose, while patch cover was held constant (e.g., at 10%). DLI and MDLI were highest (i.e., landscapes were most leaky) when patches of 25-pixel size were tightly clustered (Figure 4a). Leakiness slightly decreased as the tightness of patch clusters became less, that is, as patches became more uniformly dispersed over the map. Again, this is the logical response expected from field and modelling studies (e.g., Reynolds et al. (1997); Cross and Schlesinger (1999)). Although not shown here for brevity, this response holds for other patch sizes.

We also varied patch shape, and oriented patches to form banded configurations, which occur in many arid and semiarid lands around the world (e.g., Valentin et al. (1999)). We generated maps with elongated patches varying in length and width (from short thick bands to long narrow stripes), while holding the cover and size of patches constant (Figure 2d). For flows in the direction of columns, DLIc decreased as the shape and orientation of patches formed greater obstructions across the path of flow (Figure 4b). In other words, spatial maps with long stripes in rows obstructing flows going down columns had a lower leakiness than landscapes with short thick bands.

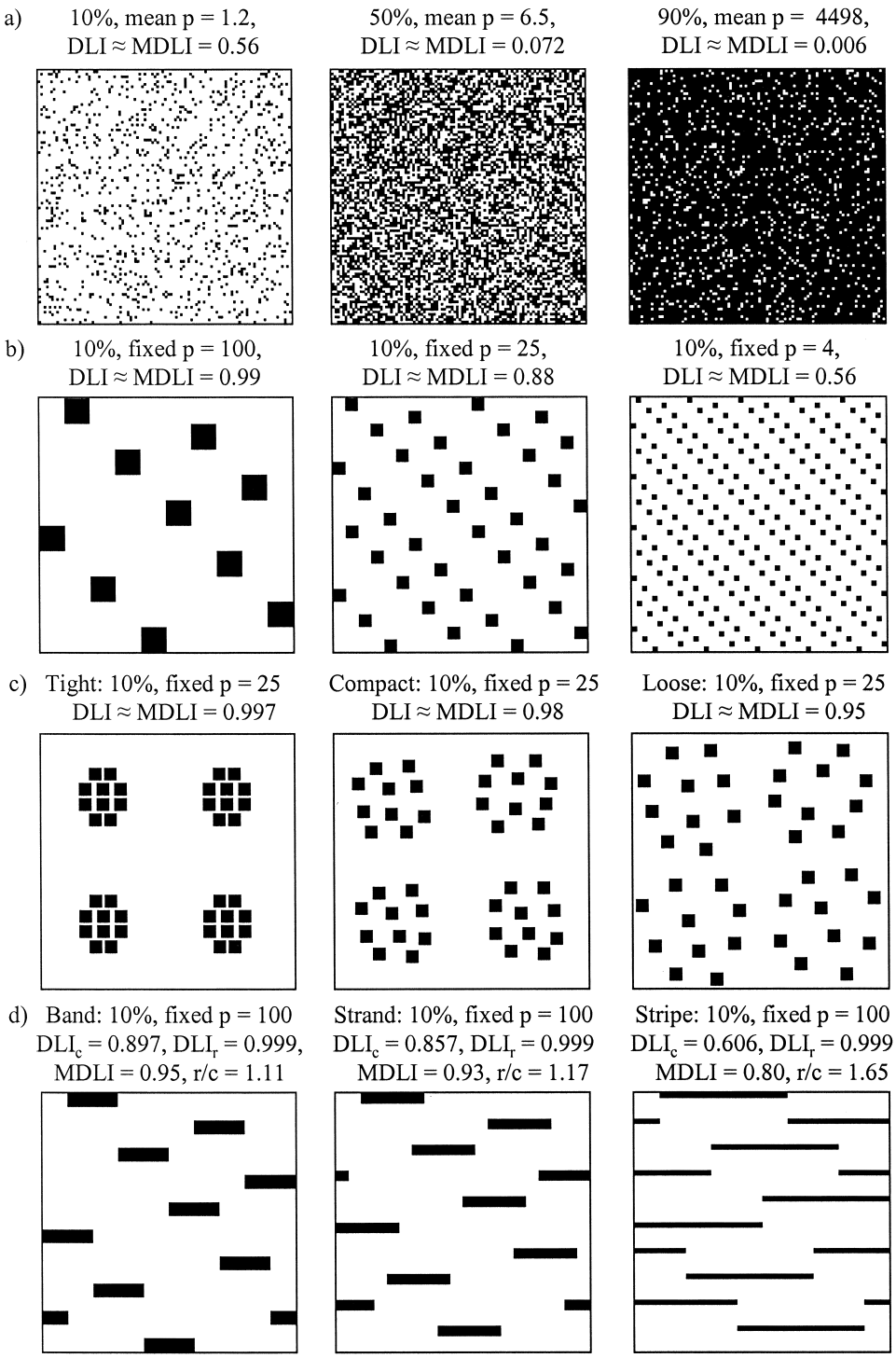

Figure 2. Examples of modelled landscape maps: a) three levels of patch cover as random patterns, b) three patch sizes as squares of patch pixels in a regular pattern, c) three patch cluster arrangements (four groups of ten patches tightly, compactly or loosely aggregated), and d) three patch shapes (bands, strands and stripes) oriented across rows. Maps are 100×100 pixels of 1 m dimension. Attributes of maps are labelled at the top as: % patch cover, patch size (in pixels, p), and DLI and MDLI [and for panel d, DLIr and the ratio of DLIr to DLIc (r/c)].

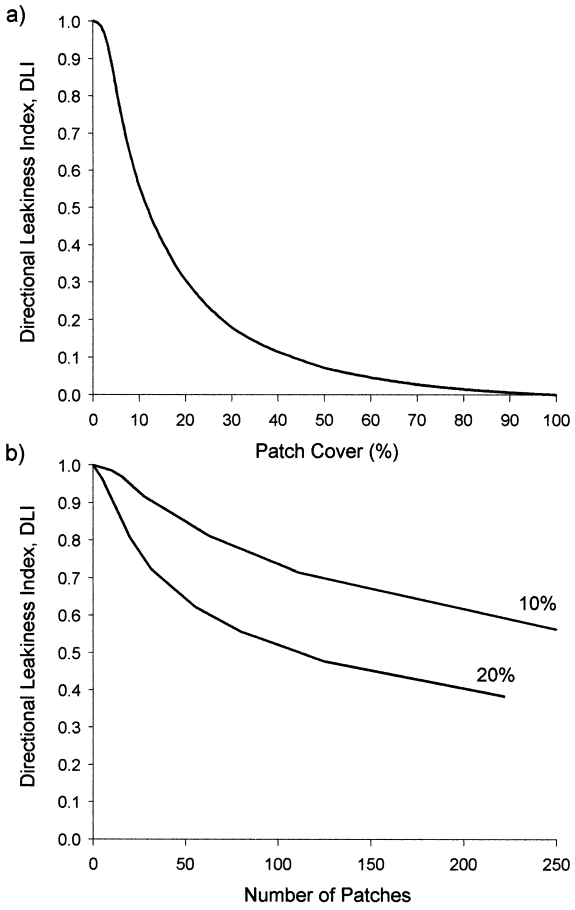

Figure 3. Changes in the directional leakiness index DLI with a) the total cover of patches formed by the random dispersion of single patch pixels, and b) the number of patches formed by a regular dispersion of increasingly smaller squares of patch pixels for 10% and 20% total patch cover.

When flows were in the direction of the banding (rows), leakiness was always very high, as expected for 10% cover.

Further, the degree of banding is indicated by the ratio of DLIr to DLIc (r/c in Figures 2d and 4b). The r/c ratio for long, overlapping stripes is greater than for short, non-overlapping bands. Also, when patch cover, size and pattern were the same, landscapes with patches shaped as bands had a lower leakiness than with patches shaped as squares (DLI = 0.897 and 0.99, left panels of Figures 2d and 2b, respectively). These results clearly demonstrated that DLI is sensitive to patch shape and orientation for a regular spatial arrangement and a low total patch cover (10%). Although not illustrated here, as patch cover increases this sensitivity decreases, as expected.

An application to savannas

The utility of DLI and MDLI for assessing the relative leakiness of natural landscapes was evaluated by using maps for three savanna landscape sites located in northern Australia (sites described in Ludwig et al. (1999b)). These sites differed in their distance from a cattle watering-point, hence, vegetation patch attributes. Site KS1 was located near this watering-point (about 75 m away) and had large open areas of bare soil with only a few patches of perennial vegetation, mostly spiny shrubs (Figure 5a). Site KS3 was located 1.4 km from water and had a cover of mostly low annual grasses (Figure 5b). Site KS5 was within an exclosure (ungrazed for 27 years) and had a high cover of perennial grass patches and some shrubs (Figure 5c).

The maps for these three landscapes were delimited within aerial videography images (details on videography in Kinloch et al. (2000); Ludwig et al. (2000b); Pickup et al. (2000)). Each pixel in these images had a dimension of approximately 0.20 m (exact pixel dimensions for each image were derived from field markers; Figure 5). Within these pixel images, maps of approximately 50 m by 20 m were delineated, that is, we selected rectangular areas of about 1,000 m^2. Thus, maps were composed of 25,000 pixels. Then, each pixel was classified into: (1) flow obstructing vegetation patches, including perennial grass clumps, tree groves and shrub thickets; and (2) non-obstructing interpatches, including open areas of bare soil, surface litter and annual plants. The classified map for site KS1, located near water, only had a few flow obstructing patches (right panel, Figure 5a), hence is likely to be very leaky. In contrast, the classified map for site KS5, located within an exclosure, is mostly patch (right panel, Figure 5c), hence is likely to be non-leaky. Site KS3, located 1.4 km from water, is intermediate in patch cover (right panel, Figure 5b) and likely leakiness.

We used DLI to assess the potential leakiness of these three landscape sites because the direction of the slope of each site was known (Ludwig et al. 1999b), but we have also included MDLI values for comparative interest. The DLI (and MDLI) for the site closest to water (KS1) was much greater than that for the site 1.4 km from water (KS3), and for the exclosure site (KS5) (Figure 6a). These results indicate that KS1 is far more likely to be leaky than the other two landscapes, as expected (compare Figures 5a with Figures 5b and 5c). Also, note that DLI and MDLI

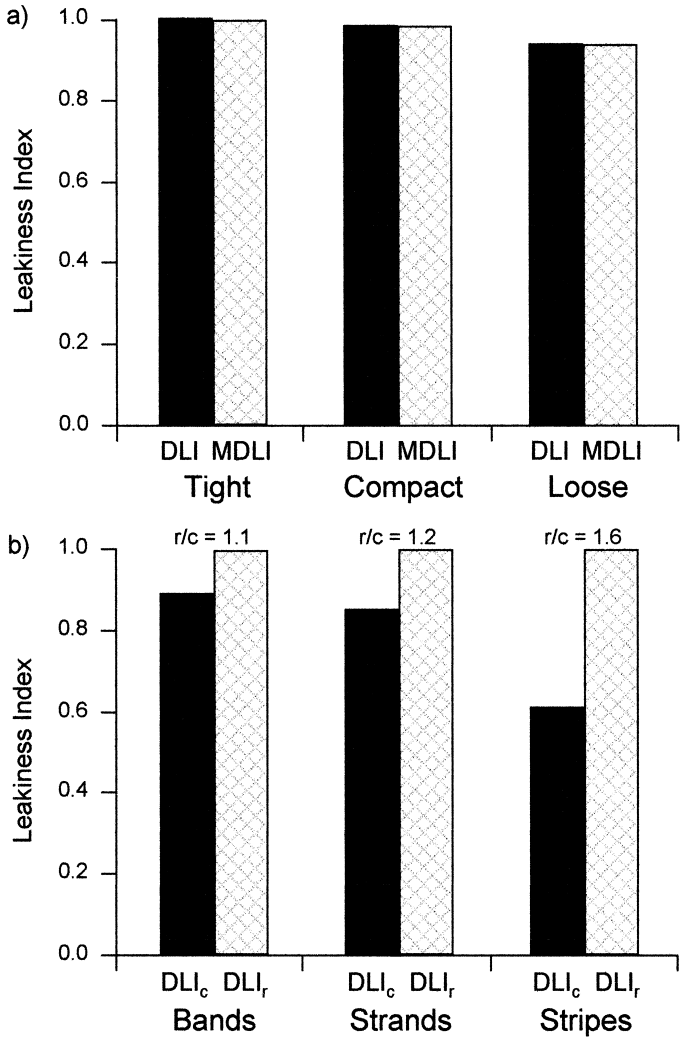

Figure 4. a) DLI and MDLI for three spatial maps differing in the degree to which patches are clustered; and b) DLI for columns, c, and rows, r (DLIc and DLIr), and their ratio (r/c), for three patch shapes: bands, strands and stripes (banding oriented across rows, see Figure 2d).

were similar (i.e. DLIr $\approx$ DLIc). Then, DLI was used to position these sites along a continuum of landscape functionality in terms of their potential to retain or conserve resources (Figure 6b).

Discussion

The directional landscape leakiness index, DLI, was derived from basic principles of landscape patterns, processes and functions. Therefore, this index is conceptually and intuitively easy to understand in terms of how landscape patch structures potentially operate to retain the limited resources that are so vital to the functioning of many desert, grassland and savanna ecosystems. We demonstrated the utility of this landscape leakiness index by comparing three semiarid savanna landscapes that differed in their remotely-sensed vegetation patch attributes (Ludwig et al. 1999b); DLI clearly separated and positioned the three landscapes along a function-dysfunction continuum of resource conservation. Of course, for DLI to be applicable, landscapes must have distinctive vegetation patches (e.g., semiarid shrublands). Equally, these patches must have the physical structures necessary to trap resources and the biological processes needed to utilise these resources to maintain patch structure and function (Tongway and Ludwig 1997a; Reynolds et al. 1999).

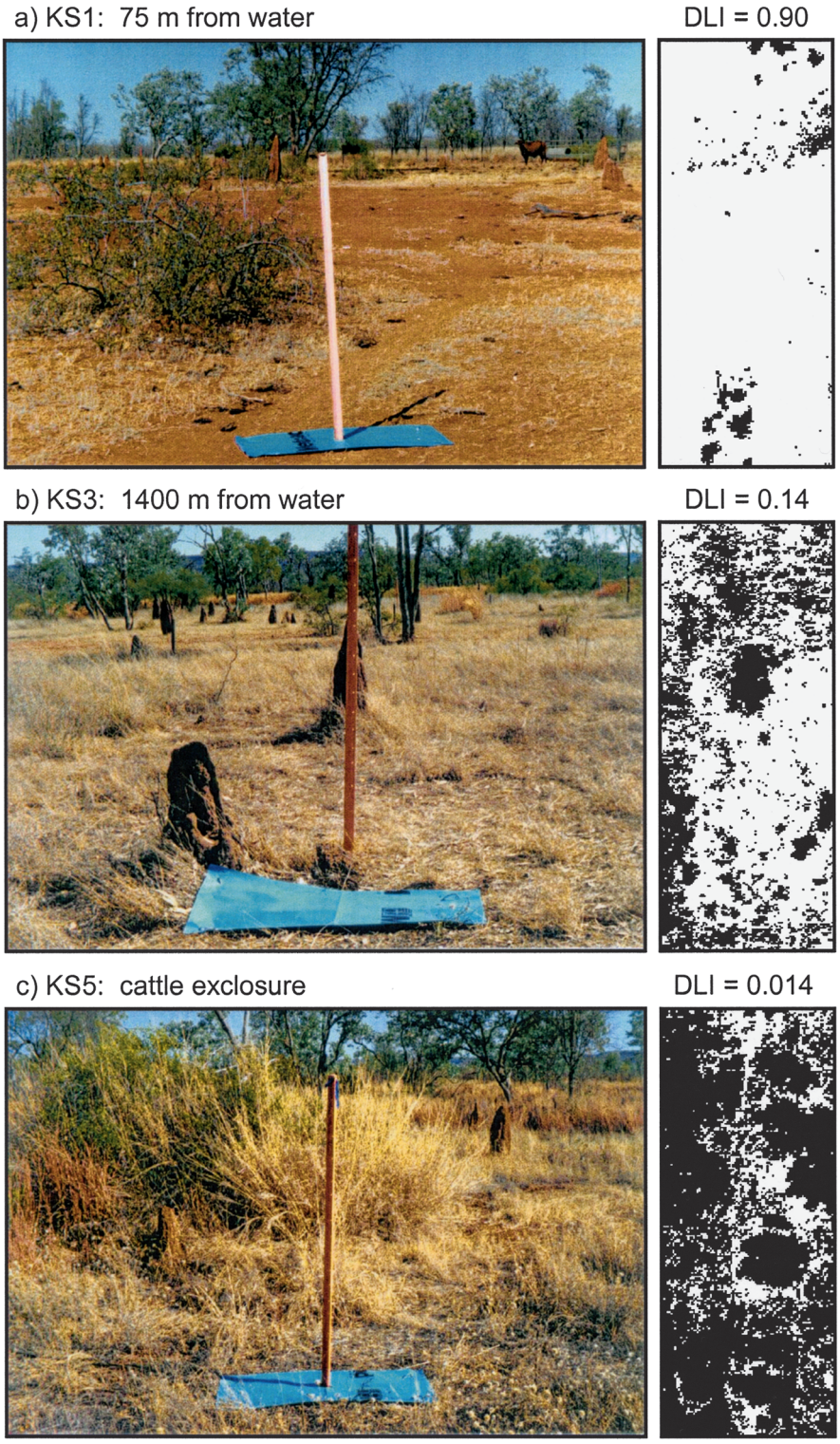

Figure 5. Photographs and classified images for three savanna landscape sites located on Kidman Springs Research Station that differ in patch attributes, hence DLI values, due to distance from a cattle watering point: a) 75 m, KS1, and b) 1.4 km, KS3, or due to being within a cattle exclosure: c) KS5. The markers in the photographs are 0.5 m by 1.0 m, and were used to calibrate the aerial videography images, which were 20 m wide by 50 m long. In the classified images patches are groups of dark pixels and interpatches are light areas. As illustrated, the top of the image is upslope and the bottom downslope (slopes < 1%).

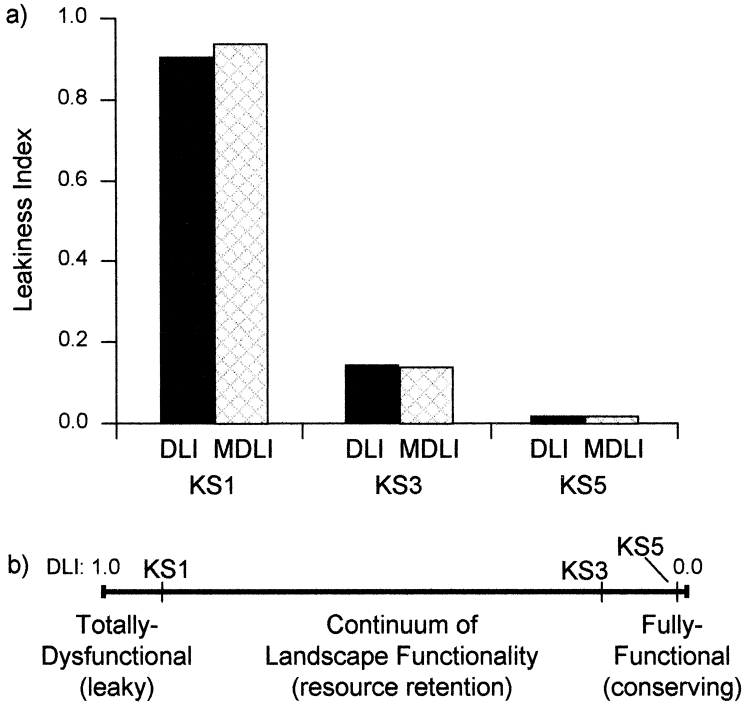

Figure 6. a) DLI and MDLI for three savanna sites differing in their distance from a cattle watering point or exclosure, hence vegetation patch attributes; and b) based on their DLI, the position of these three sites along a landscape functionality continuum (potential to retain resources).

A variant of DLI for multi-directional leakiness, MDLI, was computed as a simple average of DLIc and DLIr. However, if DLIc and DLIr are dissimilar (a statistical test for this dissimilarity needs to be developed), this implies that the shape and orientation of patches within the landscape is strongly patterned. For example, vegetation patches may form bands across the landscape (Valentin et al. 1999). If bands are along rows, a high ratio of row to column leakiness (i.e., DLIr/DLIc) would result. If banding is at an angle across the map, then the classified image could be iteratively rotated to maximize the DLIr/DLIc ratio, with the DLIc for this maximum taken as the index of leakiness rather than MDLI. However, this assumes that one is confident that the banding pattern is along rows and is related to resource flows down columns. Although this pattern-process relationship usually applies to banded vegetation, verifying this relationship requires field studies (e.g., Valentin et al. (1999)).

When comparing savanna landscapes, we used three sites with similar vegetation, soils and topography. These sites were all located in the same area, thus were subject to the same climate. When comparing the functionality of landscapes with different climates, topography, soils or vegetation, DLI or MDLI values must be interpreted more carefully. This is because arid and semiarid landscapes such as deserts, grasslands and savannas occurring in different rainfall zones and on different soils will differ in their natural vegetation patch attributes. For example, in Australian savannas, mean patch size and cover decline as rainfall increases on sands and loams but not on clays (Ludwig et al. 1999c).

One approach to making landscapes from different climates and occurring on different soils more comparable would be to scale DLI, hence MDLI, relative to a different minimum leakiness value, that is, set *Lmin* to a value greater than 0. For example, minimum leakiness could be taken as that for a undisturbed or natural landscape with a specific vegetation type, topography, soils and climate. In other words, minimum leakiness is not taken as a site with 100% patch cover assumed to completely retain resources where *Lmin* = 0, but is assigned a leakiness value based on the patch cover expected for an undisturbed landscape in a climate-terrain-soil setting. For example, *Lmin* might be set to equate to a DLI of 0.2 for an undisturbed arid shrubland setting in central Australia, such as that described by Kinloch et al. (2000).

Sites within this climate-vegetation-soil setting would then be more comparable to other settings.

For convenience, we used a rectangular shape for our remotely-sensed maps. Because our leakiness index calculation for *Lobs* uses distances down each column, *j*, of a map (Equation 2), one could use columns of variable height across an image to maximize the area of image sampled by a spatial map. If the height of columns varies considerably, DLI may need to be weighted by column height (weighted DLI is a future development).

Edge effects, which are truncation effects imposed by a map boundary (Gardner 1999), may influence *Lobs* and, hence, DLI calculations. Basically, in scaling up to a standard area, calculations assume that pixels just outside the bottom edge of a map column are the same as those at the top of the same column. These edge effects are negligible for maps with a high cover of patch pixels (e.g., >90%), but increase for sparser maps, particularly if the map area is small. If patch pixels are sparse (e.g., total patch cover <10%) so that dt_j and db_j are small compared to $\Sigma_i dp_{i,j}^2$, or if many columns have no patch pixels, then we recommend delimiting as large a map as possible within an image.

Because DLI is the sum of the squared distances for every interpatch opening down each column in a landscape map, it is weighted by the square of the length of this opening. The rationale for this power function weighting is that as water falls on, or flows down, a long open slope (Williams 1978), or as litter and soil particles are blown across a large open area (Miles and McTainsh 1994), these materials gain energy or momentum. In other words, erosion forces are far greater within larger openings in a landscape than for smaller openings – such nonlinear erosion relationships have been observed in many natural and cropped systems in arid and semiarid landscapes (e.g., Freebairn et al. (1991); Leys (1991); Tongway and Ludwig (1997a); Schlesinger et al. (2000)). These studies document that large openings in a landscape (e.g., large areas of bare soil) have a greater influence on resource redistribution (potential leakiness) than small open areas (e.g., small gaps between perennial grass clumps).

These squared interpatch distances could also be weighted by the type of patch obstructing each interpatch flow because some types of patches are more efficient at trapping and retaining resources than are other patch types. For example, a tall shrub thicket is more likely to trap wind-blown litter and soil particles than is a short-grass clump (Reynolds et al. 1997). Thus, in computing *Lobs*, differential weightings could be applied for different patch types based on an estimate of their relative efficiency in trapping specific resources. When using patch weightings to compute a weighted DLI, *Lobs*, *Lmax* and *Lmin* would also need to be appropriately weighted to keep this index in the range 0 to 1. This patch weighting could be a useful future development for DLI if there was a requirement to contrast resource leakiness in landscapes with subtle differences in patch attributes. However, sufficient information about patch trapping efficiency is not currently available and would require field studies.

The maps that we derived from aerial videography images of savannas were small-scaled (covering approximately 1,000 m^2 of landscape) and of high-resolution (pixel dimension about 20 cm). If one desires to explore landscape functionality over a greater area, then a larger image is needed. With air-borne videography, flying higher above the ground surface can capture a larger image, but for the fixed camera settings we used this will result in a coarser resolution (e.g., pixels of 1 m). Alternatively, if one wants to cover a larger area, then high-resolution satellite imagery could be used, for example, the 4-m pixel, multi-spectral (blue, green, red, near infrared) imagery of IKONOS satellites (Tanaka and Sugimura 2001). However, for any imagery to be meaningful in terms of landscape functionality for resource retention, image pixel size must be small enough to distinguish flow-obstructing patches from non-obstructing interpatch openings (e.g., areas of bare soil). In some vegetation types, such as for tussock grasslands, pixel size would need to be very small to identify such fine-grained vegetation patches (e.g., the 20 cm pixels used in this study). In more open vegetation such as semiarid woodland, where patches and open interpatch areas are larger (e.g., banded *Acacia*; Ludwig and Tongway (1995)), the 4-m pixel size of IKONOS would be adequate. Even the 30 m and larger pixel sizes of Landsat imagery can detect large vegetation patches (e.g., Pickup et al. (1993)).

Our landscape leakiness concept and index (DLI) assumes that flows are approximately in a straight-line direction. This assumption is reasonable for many low-relief Australian landscapes where sheet-flows dominate, for example, on many hillslopes in the semiarid woodlands of eastern Australia (Ludwig and Tongway 1995). However, if images include rougher terrain, such as the ranges and piedmonts in arid cen-

tral Australia (e.g., Pickup and Chewings (1996)), then flows of water are more tortuous and down channels. For such complex terrain and flows, perhaps, DLI calculations could be linked to digital elevation models and satellite imagery within a geographic information system (GIS).

Alternatively, other resource redistribution or erosion models could be used (e.g., the erosion-cell model; Pickup (1985)). However, such geomorphic/hydrologic/erosion models are complex and include many factors influencing runoff and soil erosion such as rainfall (amount and intensity), soil texture and infiltration rates, slope length, and surface cover type (e.g., Freebairn et al. (1989); Leys (1991)). Although these models may estimate soil losses quite accurately, collecting the data required by such models is costly and time consuming. Our aim in this paper was to present a new, simple index of landscape leakiness (DLI) that indicates the potential for a landscape to retain resources (i.e., not lose soil). This index only relies on having remotely-sensed images with pixels that can be classified as being either flow-obstructing patches or open non-obstructing interpatches.

Our landscape leakiness index is mechanistically similar to binary percolation or patch connectivity (habitat fragmentation) and animal dispersion models (e.g., Wiens et al. (1997); With et al. (1999); McIntyre and Wiens (2000)). However, the underlying concept and processes whereby landscapes retain (or leak) resources are very different (e.g., Ludwig and Tongway (2000)). Percolation and dispersion models typically assume random or constrained (row, column) movements for objects (organisms) to percolate or disperse through a landscape from patch to patch (suitable habitat). In contrast, landscape leakiness assumes non-patch to patch (source to sink) flows of materials (e.g., litter and soil particles) that are driven by wind and gravity, and that are directional (e.g., Wu et al. (2000)).

Advantages of DLI include: (1) it is conceptually simple, being based on source to sink flows; (2) it ranges from 0 to 1, being an estimated (observed) leakiness relative to a maximum and minimum leakiness; (3) it can be fit to field or experimental data relating resource losses (e.g., soil loss) to landscape patch attributes (e.g., cover) by adjusting the curvature parameter k; and (4) it is robust because its response curves vary logically with remotely-sensed landscape patch attributes such as cover, size and spatial orientation. These are the patch attributes known to influence how landscapes function to retain resources (Tongway and Ludwig 1997a, 1997b). Because DLI strongly reflects these attributes, it provides a simple and useful indicator of the potential for a landscape to retain resources, hence, it reflects an important ecological process (Tischendorf 2001).

Further, there is no need to group pixels into patches with delineated boundaries, as required for many landscape metrics describing fragmentation, segregation, connectivity and spatial heterogeneity and pattern (e.g., Li and Reynolds (1994); Riitters et al. (1995); Jaeger (2000); Wu et al. (2000); He et al. (2000); Wu and Sui (2001)). DLI only requires that each map pixel be classified as being either a flow obstructing patch (e.g., a clump of perennial vegetation) or a non-obstructing interpatch (e.g., an open area of bare soil). However, there remains a need to compare DLI with other landscape metrics (e.g., lacunarity) in terms of their relative usefulness as indicators of landscape function (a forthcoming paper).

Acknowledgements

The support of the Tropical Savannas Cooperative Research Centre is gratefully acknowledged. We sincerely thank Alan Andersen, Diane Pearson and two anonymous reviewers for suggesting ways to improve an earlier manuscript.

Appendix

Appendix A. Leakiness index calculations

To illustrate the calculation of the directional leakiness index, DLI, we use the example of a spatial map shown in Figure 1b. This map is assumed to be 20 m×20 m in size, composed of 400 1-m square pixels. We also assume that the flow direction (slope) is known and map columns are oriented in this direction of flow. We use a 100 m×100 m (1 ha) map as the standard area to scale DLI. This 1 ha standard area can be visualized as being composed of 25 of our 20 m×20 m maps. We compute a DLI for this 20 m×20 m map as scaled to 1 ha standard. However, we only illustrate detailed calculations using the first column of the map, as calculations for other columns are repetitive. We first define the distances in column 1 needed to compute the terms in Equation (2). These are the terms required to compute *Lobs* scaled to the

1 ha standard area. This is followed by definitions for *Lmax* and *Lmin*, which together with *Lobs*, are used to compute DLI.

Distances and Lobs *for column 1*

Starting at the top of column *1* in the spatial map (left-most column, Figure 1b), the distance from the top edge of the map to the first patch pixel, dt_1, is 3 m (3 interpatch pixels). At the bottom of this first column, a second edge distance, db_1, is 2 m. The distances *between* patches in this first column are $dp_{1,1}$ = 3 m, $dp_{2,1}$ = 2 m, and $dp_{3,1}$ = 2 m.

These two edge and three interpatch distances are squared, scaled and summed in a series of terms to calculate an observed leakiness for this first column, $Lobs_1$, using Equation (2): $Lobs_1 = [(h_s/h_1)\cdot(\Sigma_i dp_{i,1}^2) + ((h_s/h_1) - 1)\cdot((dt_1 + db_1)^2) + (dt_1^2 + db_1^2)]\cdot(w_s/w_m)\cdot(pd)$, where for our 20 m×20 m spatial map, h_1 = 20 and w_m = 20; for our 100 m×100 m standard area, h_s = 100 and w_s = 100; and the pixel dimension, pd = 1 m.

The first term in this equation, $(h_s/h_1)\cdot(\Sigma_i dp_{i,1}^2)$, is the non-edge component of $Lobs_1$, that is, the sum of all the squared distances between patches $(\Sigma_i dp_{i,1}^2)$ scaled by the proportional height of column 1 relative to the column height of our standard area (h_s/h_1). For column 1 of our map (Figure 1b), this non-edge term is: $(100/20)\cdot(3^2 + 2^2 + 2^2) = (5)\cdot(17) = 85$.

The second term, $((h_s/h_1)-1)\cdot((dt_1 + db_1)^2)$, is the combined-edges component of $Lobs_1$, that is, distances that are no longer edge but have become interpatch distances due to the process of scaling up. In other words, as we scale up the first 20 m×1 m column in our spatial map (Figure 1b) to the first column of our 100 m×100 m standard area, the pattern of pixels in the 20 m column is repeated in pixels 21–40, 41–60, 61–80 and 81–100. In doing so, the bottom edge in the first 20 m (i.e. db_1) will now be joined to the top edge in the second 20 m (i.e. dt_1) to form a new interpatch distance (i.e., $dp_{i,1} = db_1 + dt_1$). There are four of these new distances, defined by $(h_s/h_1)-1 = (100/20)-1 = 4$. Thus, this combined-edges term is: $(4)\cdot(2 + 3)^2 = (4)\cdot(25) = 100$.

The third term, $(dt_1^2 + db_1^2)$, is the remaining-edges component, that is, the distances in the first column of our 100 m×100 m standard area that are still edges. This remaining-edges term is: $(3^2 + 2^2) = 13$.

These three terms are now summed and scaled by the proportional width of the sample map (w_s/w_m) and the pixel dimension (pd, in meters) to obtain:

$$\begin{aligned} Lobs_1 &= (85 + 100 + 13)\cdot(100/20)\cdot(1) \\ &= (198)\cdot(5)\cdot(1) \\ &= 990. \end{aligned}$$

These calculations are then repeated for all 20 columns of the spatial map (Figure 1b) and summed from j = 1 to 20 to obtain an *Lobs* for our spatial map that is scaled to the standard area:

$$Lobs = \sum_j (Lobs_j) = 21{,}065$$

Lmax, Lmin *and computing DLI*

Lmax represents a maximally leaky standard area defined as having columns with no flow-obstructing patch pixels. For our 100 m×100 m standard area, this $Lmax = (h_s)^2\cdot w_s = (100)^2\cdot 100 = 1{,}000{,}000$.

In contrast, *Lmin* represents a minimally leaky standard area defined as having columns fully occupied by flow-obstructing patch pixels that have no leakiness. Thus, for an area full of such patch pixels, *Lmin* = 0.

Then, using *Lobs*, *Lmax* and *Lmin* components in Equation (1), the DLI for our 20 m×20 m spatial map (Figure 1b), scaled to a 1 ha standard area, is:

$$DLI = 1 - [(L_{max_1} - L_{obs_1})/(L_{max_1} - L_{min_1})]^k$$

$$\begin{aligned} DLI &= 1 - [(1{,}000{,}000 - 21{,}065)/(1{,}000{,}000 - 0)]^5 \\ &= 1 - (978{,}935/1{,}000{,}000)^5 \end{aligned}$$

$$DLI = 1 - (0.979)^5 = 1 - 0.899 = 0.101.$$

This leakiness value of 0.101 is interpreted relative to a 0 for no leakiness and to 1 for totally leakiness. This indicates that our spatial map is not likely to be leaky.

Programs for computing DLI, and its variant MDLI, are available upon request from authors as a Microsoft 'Windows' 32-bit application with user interface and image display (AL) or as a Fortran executable code that can be used for batch processing (VC).

References

Anderson V.J. and Hodgkinson K.C. 1997. Grass-mediated capture of resource flows and the maintenance of banded mulga in a semiarid woodland. Australian Journal of Botany 45: 331–342.

Burke I.C., Lauenroth W.K., Riggle R., Brannen P., Madigan B. and Beard S. 1999. Spatial variability of soil properties in the shortgrass steppe: the relative importance of topography, grazing, microsite, and plant species in controlling spatial patterns. Ecosystems 2: 422–438.

Carroll C. and Tucker A. 2000. Effects of pasture cover on soil erosion and water quality on central Queensland coal mine rehabilitation. Tropical Grasslands 34: 254–262.

Cross A.F. and Schlesinger W.H. 1999. Plant regulation of soil nutrient distribution in the northern Chihuahuan Desert. Plant Ecology 145: 11–25.

Findlater P.A., Cater D.J. and Scott W.D. 1990. A model to predict the effects of prostrate ground cover on wind erosion. Australian Journal of Soil Research 28: 609–622.

Freebairn D.M., Silburn D.M. and Loch R.J. 1989. Evaluation of three soil erosion models for clay soils. Australian Journal of Soil Research 27: 199–211.

Freebairn D.M., Littleboy M., Smith G.D. and Coughlan K.J. 1991. Optimising soil surface management in response to climatic risk. In: Muchow R.C. and Bellamy J.A. (eds), Climatic Risk in Crop Production: Models and Management for the Semiarid Tropics and Subtropics. CAB International, Wallingford, UK, pp. 283–305.

Galle S., Ehrmann M. and Peugeot C. 1999. Water balance in a banded vegetation pattern: A case study of tiger bush in western Niger. Catena 37: 197–216.

Gardner R.H. 1999. RULE: map generation and a spatial analysis program. In: Klopatek J.M. and Gardner R.H. (eds), Landscape Ecological Analysis: Issues and Applications. Springer, New York, NY, USA, pp. 280–303.

He H.S., DeZonia B.E. and Mladenoff D.J. 2000. An aggregation index (*AI*) to quantify spatial patterns of landscapes. Landscape Ecology 15: 591–601.

Jaeger J.A.G. 2000. Landscape division splitting index and effective mesh size: new measures of landscape fragmentation. Landscape Ecology 15: 115–130.

Johns G.G. 1983. Runoff and soil loss in a semi-arid shrub invaded poplar box (*Eucalyptus populnea*) woodland. Australian Rangeland Journal 5: 3–12.

Kinloch J.E., Bastin G.N. and Tongway D.J. 2000. Measuring landscape function in chenopod shrublands using aerial videography. In: Proc. 10th Australian Remote Sensing Conference, Proceedings published on CD-ROM., Adelaide, Australia.

Lang R.D. and McCaffrey L.A.H. 1984. Ground cover – its effects on soil loss from grazed runoff plots, Gunnedah. Journal of Soil Conservation New South Wales 40: 56–61.

Leys J.F. 1991. Towards a better model of the effect of prostrate vegetation cover on wind erosion. Vegetatio 91: 49–58.

Li B-L. and Archer S. 1997. Weighted mean patch size: a robust index for quantifying landscape structure. Ecological Modelling 102: 353–361.

Li H. and Reynolds J.F. 1994. A simulation experiment to quantify spatial heterogeneity in categorical maps. Ecology 75: 2446–2455.

Ludwig J.A. and Tongway D.J. 1995. Spatial organisation of landscapes and its function in semi-arid woodlands Australia. Landscape Ecology 10: 51–63.

Ludwig J.A. and Tongway D.J. 2000. Viewing rangelands as landscape systems. In: Arnalds O. and Archer S. (eds), Rangeland Desertification. Kluwer Academic Publishers, Dordrecht, The Netherlands, pp. 39–52.

Ludwig J.A., Tongway D.J. and Marsden S.G. 1999a. Stripes, strands or stipples: modelling the influence of three landscape banding patterns on resource capture and productivity in semi-arid woodlands, Australia. Catena 37: 257–273.

Ludwig J.A., Eager R.W., Williams R.J. and Lowe L.M. 1999b. Declines in vegetation patches, plant diversity, and grasshopper diversity near cattle watering-points in the Victoria River District, northern Australia. Rangeland Journal 21: 135–149.

Ludwig J.A., Tongway D.J., Eager R.W., Williams R.J. and Cook G.D. 1999c. Fine-scale vegetation patches decline in size and cover with increasing rainfall in Australian savannas. Landscape Ecology 14: 557–566.

Ludwig J.A., Wiens J.A. and Tongway D.J. 2000a. A scaling rule for landscape patches and how it applies to conserving soil resources in savannas. Ecosystems 3: 84–97.

Ludwig J.A., Bastin G.N., Eager R.W., Karfs R., Ketner P. and Pearce G. 2000b. Monitoring Australian rangeland sites using landscape function indicators and ground- and remote-based techniques. Environmental Monitoring and Assessment 44: 167–178.

McIntyre N.E. and Wiens J.A. 2000. A novel use of the lacunarity index to discern landscape function. Landscape Ecology 15: 313–321.

McIvor J.G., Williams J. and Gardener C.J. 1995. Pasture management influences runoff and soil movement in the semi-arid tropics. Australian Journal of Experimental Agriculture 35: 55–65.

Miles J.R. and McTainsh G.H. 1994. Wind erosion and land management in the mulga lands of Queensland. Australian Journal of Soil & Water Conservation 7: 41–45.

Pickup G. 1985. The erosion cell – a geomorphic approach to landscape classification in range assessment. Australian Rangeland Journal 7: 114–121.

Pickup G. and Chewings V.H. 1996. Correlations between DEM-derived topographic indices and remotely-sensed vegetation cover in rangelands. Earth Surface Processes and Landforms 21: 517–529.

Pickup G., Chewings V.H. and Nelson D.J. 1993. Estimating changes in vegetation cover over time in arid rangelands using Landsat MSS data. Remote Sensing of Environment 43: 243–263.

Pickup G., Bastin G.N. and Chewings V.H. 2000. Measuring rangeland vegetation with high resolution airborne videography in the blue-near infrared spectral region. International Journal of Remote Sensing 21: 339–351.

Pressland A.J. and Lehane K.J. 1982. Runoff and the ameliorating effect of plant cover in the mulga communities of south western Queensland. Australian Rangeland Journal 4: 16–20.

Reynolds J.F., Virginia R.A. and Schlesinger W.H. 1997. Defining functional types for models of desertification. In: Shugart H.H., Smith T.M. and Woodward F.I. (eds), Plant Functional Types: Their Relevance to Ecosystem Properties and Global Change. Cambridge Univ Press, Cambridge, UK, pp. 195–216.

Reynolds J.F., Virginia R.A., Kemp P.R., De Soyza A.G. and Tremmel D.C. 1999. Impact of drought on desert shrubs: effects of seasonality and degree of resource island development. Ecological Monographs 69: 69–106.

Reid K.D., Wilcox B.P., Breshears D.D. and MacDonald L. 1999. Runoff and erosion in a Piñon-Juniper Woodland: influence of vegetation patches. Soil Science Society of America Journal 63: 1869–1879.

Riitters K.H., O'Neill R.V., Hunsaker C.T., Wickham J.D., Yankee D.H., Timmins S.P. et al. 1995. A factor analysis of landscape pattern and structure metrics. Landscape Ecology 10: 23–39.

Scanlan J.C., Pressland A.J. and Myles D.J. 1996. Run-off and soil movement on mid-slopes in north-east Queensland grazed woodlands. Rangeland Journal 18: 33–46.

Schlesinger W.H., Ward T.J. and Anderson J. 2000. Nutrient losses in runoff from grassland and shrubland habitats in southern New Mexico: II. field plots. Biogeochemistry 49: 69–86.

SPSS Inc. 2000. SigmaPlot 2000 Programming Guide. SPSS Science Marketing, Chicago, IL, USA.

Tanaka S. and Sugimura T. 2001. A new frontier of remote sensing from IKONOS images. International Journal of Remote Sensing 22: 1–5 (in press).

Tischendorf L. 2001. Can landscape indices predict ecological processes consistently? Landscape Ecology 16: 235–254.

Tongway D.J. and Ludwig J.A. 1997a. The conservation of water and nutrients within landscapes, Chapter 2. In: Ludwig J., Tongway D., Freudenberger D., Noble J. and Hodgkinson K. (eds), Landscape Ecology Function and Management: Principles from Australia's Rangelands. CSIRO Publishing, Melbourne, Australia, pp. 13–22.

Tongway D.J. and Ludwig J.A. 1997b. The nature of landscape dysfunction in rangelands, Chapter 5. In: Ludwig J., Tongway D., Freudenberger D., Noble J. and Hodgkinson K. (eds), Landscape Ecology, Function and Management: Principles from Australia's Rangelands. CSIRO Publishing, Melbourne, Australia, pp. 49–61.

Valentin C., d'Herbes J.M. and Poesen J. 1999. Soil and water components of banded vegetation patterns. Catena 37: 1–24.

Whisenant S.G. 1999. Repairing Damaged Wildlands: A Process-Oriented, Landscape-Scale Approach. Cambridge Univ Press, Cambridge, UK.

Wiens J.A., Schooley R.L. and Weeks R.D. 1997. Patchy landscapes and animal movements: do beetles percolate? Oikos 78: 257–264.

Williams M.A.J. 1978. Water as an eroding agent. In: Howes K.M.W. (ed.), Studies of the Australian Arid Zone. III. Water in Rangelands. CSIRO Publishing, Melbourne, Australia, pp. 79–89.

With K.A., Cadaret S.J. and Davis C. 1999. Movement responses to patch structure in experimental fractal landscapes. Ecology 80: 1340–1353.

Wu X.B. and Sui D.Z. 2001. An initial exploration of a lacunarity-based segregation measure. Environment and Planning B: Planning and Design 28: 433–446.

Wu X.B., Thurow T.L. and Whisenant S.G. 2000. Fragmentation and changes in hydrologic function of tiger bush landscapes, south-west Niger. Journal of Ecology 88: 790–800.